

Calculated photoionization cross sections for SF₆

Harry J. Levinson, T. Gustafsson, and Paul Soven

Department of Physics and the Laboratory for Research on the Structure of Matter, University of Pennsylvania, Philadelphia, Pennsylvania 19104

(Received 14 July 1978)

We have calculated the photoionization cross sections for the valence levels of SF₆, using multiple-scattering $X\alpha$ methods for both the initial and final states. The theoretical curves are compared with measured cross sections in an attempt to complete the identification of observed photoionization peaks with theoretically predicted valence levels. We find general agreement between theory and experiment, although one notable difficulty remains.

I. INTRODUCTION

In this paper we present and discuss a series of calculations of the photoionization cross sections from the valence levels of SF₆. The primary motivation for this work was the idea that detailed comparison between measured cross sections and theoretically predicted ones would be useful in completing the identification of peaks in the photoionization spectrum of the SF₆ molecule. In this regard, we were partially successful. As a practical matter, the accuracy of the theoretical methods employed was sufficient to allow unique identification of most, but not all, of the measured photoionization peaks.

The general nature of the valence-hole spectrum of SF₆ is best discussed with the molecular-orbital diagram shown in Fig. 1.^{1,2} Group theoretical considerations determine the atomic origins and symmetries of the one-electron levels in the O_h point group of the molecule. The valence levels of sulfur and fluorine combine to form seven energy levels in the molecule. The relative ordering of these levels cannot be determined by symmetry considerations alone; in Fig. 1 the levels are drawn in accordance with the assignments made by Gustafsson.³

The partial-photoionization-cross-section data with which we are going to compare our calculations are acquired in the form of photoelectron-energy distribution curves (EDC's). These are obtained by fixing the energy of the incident photon beam and measuring the number of emitted electrons as a function of their kinetic energy. Eigenstates of the residual ion give rise to peaks in the EDC's. If one knows from another experiment the total photoionization cross section (that is, the photoabsorption cross section times the ionization probability), the partial-photoionization cross section is obtained trivially from the EDC.

Some typical EDC's are displayed in Fig. 2 (Ref. 3) and show only six peaks in the valence region.

(There is a splitting of one peak around 21.2 eV photon energy, but at no other energies. This has been attributed to autoionization.³) Throughout this paper we label the photoionization peaks as shown in Fig. 2.

The assignment of molecular orbitals to peaks in the photoelectron spectra is usually accomplished by comparing theoretically computed electron binding energies to the measured ionization potentials. The utility of this method is limited by the accuracy of the calculations, which may be of the same order as the energy separations of two ionization potentials. Such a situation is exemplified by molecular SF₆.

The core-hole spectrum of SF₆ has been measured by several groups^{4,5} and discussed theoretically by Dehmer¹ and Sachenko *et al.*⁶ For final state energies within 30 eV of threshold the spectra are dominated by two strong peaks occurring at fixed photoelectron kinetic energy. Using symmetry arguments, Dehmer inferred that these peaks are caused by the existence of final state (scattering) resonances of t_{2g} and e_g symmetry. To some degree, these can be traced back to virtual sulfur d -levels, split in the octahedral symmetry of the molecular field. In a brief report, Sachenko *et al.*⁶ described multiple scattering $X\alpha$ (MS- $X\alpha$) calculations, presumably along the lines of Dill and Dehmer,⁷ and Davenport⁸ which confirmed Dehmer's assignment.¹ The cross sections calculated by these investigators were in general agreement with the data.

Three peaks in the EDC's shown in Fig. 2 exhibit strong enhancements when the photoelectron kinetic energy is close to 5 eV, which is roughly the energy of the t_{2g} resonance present in the core spectra. Gustafsson assumed that these enhancements were the result of coupling to this resonance (or to some resonance of even parity, presumably the t_{2g}). The presumed even symmetry of the final state resonance means that only odd-parity initial states can couple to it. This assumption was in-

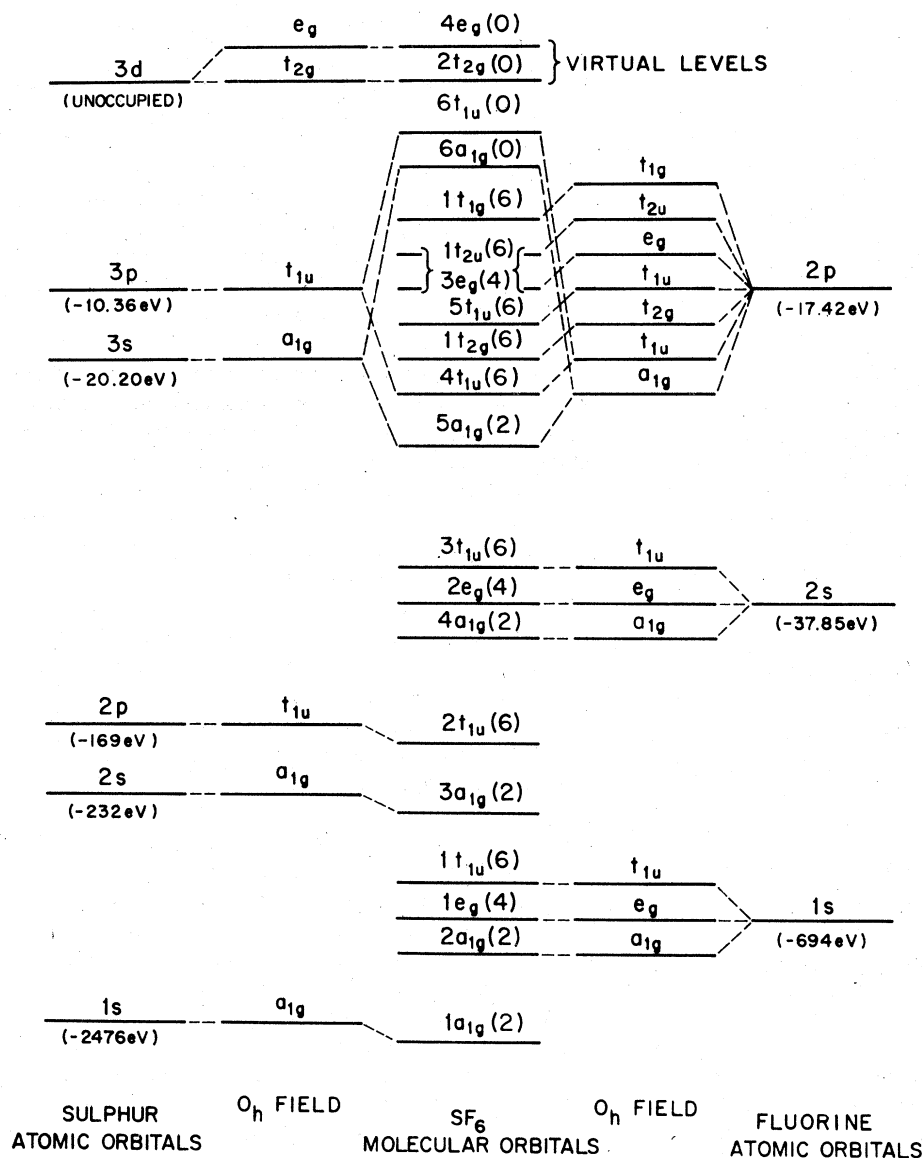


FIG. 1. Molecular-orbital (MO) diagram for SF_6 . The ground-state occupation numbers of the MO's are given in parentheses. The atomic binding energies for the constituent atoms²³ are also shown.

strumental in allowing the assignment of peak 5 to $4t_{1u}$, and peaks 2 and 3 to $1t_{2u}$ and $5t_{1u}$, in some order.³ This assignment is reasonable as calculations of binding energies give an unambiguous (in any event, uncontested) ordering for $4t_{1u}$ and $(1t_{2u}, 5t_{1u})$.⁹⁻¹⁴ It was somewhat more difficult to assign the even-parity initial states.

Ground-state calculations have not led to a consensus regarding the complete ordering of the even-parity states; nevertheless, these calculations have provided a partial ordering, dividing the even-parity states into two groups: ($5a_{1g}$, $1t_{2g}$) at higher binding energy and ($3e_g$, $1t_{1g}$).

Peak 6 is strong in the electron spectroscopy for chemical analysis (ESCA) spectrum and presum-

ably arises from a level with appreciable s-character; the molecular-orbital diagram suggests that it must be due to emission from the $5a_{1g}$ level. By elimination, peak 4 was assigned to $1t_{2g}$. The remaining even-parity states pose a difficult problem. On the basis of intensity, peak 1 was assigned $1t_{1g}$, and peak 2 was assumed (in agreement with some, but not all, earlier work) to be a doublet arising from $3e_g$ as well as either $1t_{2u}$ or $5t_{1u}$.³

II. METHOD OF CALCULATION

The partial-photoionization cross sections of SF_6 were calculated using multiple scattering $X\alpha$

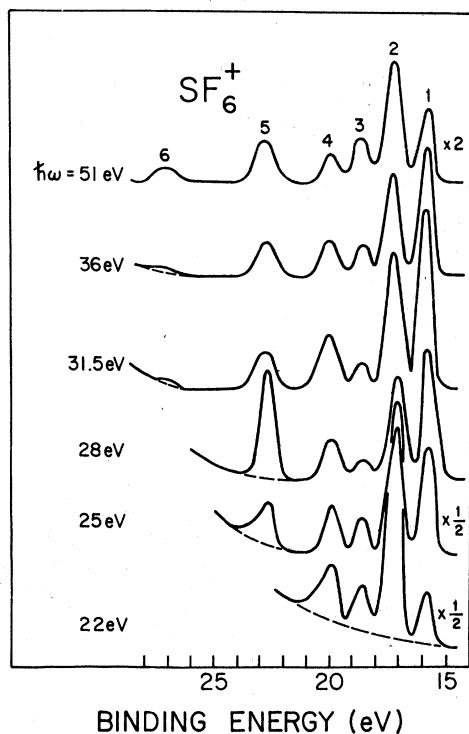


FIG. 2. Representative energy-distribution curves for SF₆⁺ valence levels, taken from the work of Gustafsson.³

techniques. The details of ground-state calculations using these methods are discussed in review articles by Slater¹⁵ and Johnson.¹⁶ Dill and Dehmer,⁷ and Davenport⁸ have discussed its application to the calculation of photoemission cross sections.

In *MS-X α* , exchange and correlation energies are approximated by a self-consistently-determined local potential given by $-e\alpha[(3/8\pi)n(\vec{r})]^{1/3}$, where $n(\vec{r}) = \sum n_i \psi_i^*(\vec{r})\psi_i(\vec{r})$ is the electron density. n_i is the occupation number of the molecular orbital ψ_i (normalized to unity), and α is a parameter of the calculation. Thus, the potential- and initial-state wave functions are found by self-consistently solving the following equations:

$$[(-\hbar^2/2m)\nabla^2 + V_\alpha(\vec{r})]\psi_i(\vec{r}) = \epsilon_i \psi_i(\vec{r}), \quad (1a)$$

$$V_\alpha(\vec{r}) = - \sum_j \frac{Z_j e^2}{|\vec{r} - \vec{R}_j|} + e^2 \sum_i n_i \int \frac{\psi_i^*(\vec{r}')\psi_i(\vec{r}')}{|\vec{r} - \vec{r}'|} d\vec{r}' - 3e^2 \alpha \left[\frac{3}{8\pi} \sum_i n_i \psi_i(\vec{r})\psi_i^*(\vec{r}) \right]^{1/3}, \quad (1b)$$

where Z_j is the nuclear charge for the atom at position \vec{R}_j . The ϵ_i are the *X- α* eigenvalues and are not one-electron binding energies, though they do have the units of energy. This is similar to the situation in Hartree-Fock theory. One may obtain

eigenvalues which are electron binding energies by doing a "transition state" calculation.^{15,16} This involves decreasing the occupation number by one-half for the state whose binding energy is desired. Since the *MS-X α* method involves only the electron density, nonintegral numbers of electrons do not pose a problem. In our calculations, only the valence levels were varied during the self-consistency procedure, while the fluorine 1s and the sulfur 1s, 2s, and 2p energies were "frozen" at Herman-Skillman atomic eigenvalues.¹⁷ Spin-orbit effects were not included.

The starting potential for the iterative procedure leading to self-consistency is comprised of overlapping atomic orbitals. Herman-Skillman atomic charge densities are placed at appropriate positions in the molecule. The charge densities are summed at each point in space and then spherically averaged within each muffin-tin sphere and volume averaged in the intersphere region.

A local potential which is proportional to the one-third power of the charge density was first derived as an approximation to the exchange term in the Hartree-Fock equations.¹⁷ Hence, the method for choosing α frequently requires agreement between *X- α* and Hartree-Fock in some sense. One may, for example, require that the two methods yield the same total energy. Alternatively, since our work is primarily concerned with matrix elements involving wave functions rather than energy eigenvalues, a procedure which produces a more accurate wave function is preferred. For this reason we have employed the α values suggested by Schwarz,¹⁸ which produce orbitals satisfying the virial theorem when they are inserted into Hartree-Fock equations. The single atom α values are used in the atomic spheres for SF₆. In the intersphere region we employed $\alpha_{\text{inter}} = \frac{1}{3}(6\alpha_F + \alpha_S)$, while for the outer sphere, $\alpha_{\text{out}} = \alpha_F$. The parameters of the calculation are given in Table I. None of these parameters were varied in order to improve agreement between data and calculation.

A muffin-tin approximation is used. The muffin-

TABLE I. Parameters of the calculation.

S-F bond distance	1.580 Å (2.986 a.u.)
S sphere radius ^a	0.932 Å
F sphere radius ^a	0.648 Å
α_S	0.724 26
α_F	0.736 51
$\alpha_{\text{out}} = \alpha_F$	0.736 51
α_{inter}^b	0.734 76
V_{inter}	-15.84 eV

^aThe covalent radii of S and F are 1.04 and 0.64 Å, respectively.

^b $\alpha_{\text{inter}} = \frac{1}{3}(6\alpha_F + \alpha_S)$.

tin radii are those used in the calculation of Connolly and Johnson,¹³ who have done a $MS-X\alpha$ ground-state calculation for SF_6 . This approximation is believed to be rather suitable for the relatively close-packed geometry of SF_6 . The value of the potential in the intersphere region V_{inter} is given in Table I. We employ a simple model in which a fixed potential is found by a self-consistent procedure involving only the ground state of the molecule. A potential constructed from the ground-state orbitals falls off exponentially at large distances from the molecule, which is, of course, appropriate for a neutral molecule. The potential used to find the wave function of outgoing photoelectron should instead fall off as $-e^2/r$ at large r . Therefore, the potential used in our calculation is modified from that of the neutral molecule so that at large r it is either $X-\alpha$ or Coulombic, whichever is stronger.¹⁹ This provides a continuous potential and the necessary asymptotic behavior. Both the initial and final states involved in the photoemission matrix element are calculated using this modified potential.

The wave functions are constructed using standard multiple scattering techniques.^{15,16} Thus, in each sphere the wave functions are expanded in terms of spherical harmonics. For the fluorine spheres, $l=0, 1$, and 2 partial waves were included for the initial-state wave function and $l=0-3$ in the final state. For the sulphur sphere and the outer sphere $l=0-4$ and $l=0-6$ were chosen for the initial and final states, respectively. Calculations using only partial waves $l=0-2$ on all spheres yielded eigenvalues shifted $\sim 2\%$, usually towards higher-binding energy, from the values listed in Table II. This, together with the good agreement with previous work using the same method,¹³ indicate a quite reasonable degree of convergence.

The photoionization cross section for a molecule of fixed orientation in a photon field is simply the transition probability per unit time from the

initial to the final states, divided by the incident-photon flux and summed over all final states. Using the Golden Rule, one obtains

$$\frac{d^2\delta}{d\Omega d\omega} = \sum \left(\frac{e^2}{\hbar c} \right) |\langle f | \vec{e}_A \cdot \vec{p} | i \rangle|^2 \frac{k}{2\pi m \hbar \omega}, \quad (2)$$

where $\hbar^2 k^2/2m = \epsilon_f$ is the kinetic energy of the outgoing electron, $\hbar\omega$ is the photon energy \vec{e}_A is the polarization of the incident radiation and \vec{p} is the momentum operator. Since the orbitals in this calculation are derived from a local potential the acceleration form for the matrix element may be used:

$$\langle f | \vec{e}_A \cdot \vec{p} | i \rangle = \frac{\hbar}{\epsilon_f - \epsilon_i} \langle f | \vec{e}_A \cdot \nabla V(\vec{r}) | i \rangle, \quad (3)$$

where ϵ_i and ϵ_f are the $X-\alpha$ eigenvalues of the initial state and final states, respectively.

Averaging Eq. (2) over all molecular orientations yields the gas-phase cross sections for polarized incident light:

$$\frac{d^2\sigma}{d\Omega d\omega} = \frac{\sigma_0}{4\pi} [1 + \beta P_2(\cos \Theta)], \quad (4)$$

where σ_0 is the angle-integrated cross section, P_2 is the second-order Legendre polynomial, $\beta = \beta(E)$ is the asymmetry parameter, and Θ is the angle of photoelectron emission measured with respect to the incident electric field.

The one-electron eigenvalues ϵ_i calculated in the $X\alpha$ approximation are not even in principle equal to the measured ionization energies. In order to fix the photon energy used in Eq. (2), for a given final-state kinetic energy, the relationship

$$\epsilon_f = \hbar^2 k^2/2m = \hbar\omega - I$$

is used instead, where I is the experimental ionization potential. The $X-\alpha$ eigenvalues, ϵ_f and ϵ_i , are used in Eq. (3), as required by the model.

III. RESULTS AND DISCUSSION

The $X-\alpha$ eigenvalues for the valence states, as calculated from the potential with the Coulomb

TABLE II. Eigenvalues and binding energies of the valence levels in SF_6 .

Valence state	$X\alpha$ Eigenvalues (present work) (eV)	$X\alpha$ Eigenvalues (Connolly and Johnson) (eV)	Transition-state energies (Connolly and Johnson) (eV)	Experimental (Gustafsson)
$1t_{1g}$	-12.25	-12.10	-15.88	-15.7
$1t_{2u}$	-13.26	-13.08	-16.84	-16.9
$5t_{1u}$	-13.36	-13.03	-16.76	-18.3
$3e_g$	-13.84	-13.76	-17.52	-16.9
$1t_{2g}$	-14.96	-15.04	-18.74	-19.8
$4t_{1u}$	-18.16	-18.09	-21.84	-22.7
$5a_{1g}$	-23.56	-22.96	-26.74	-27.0

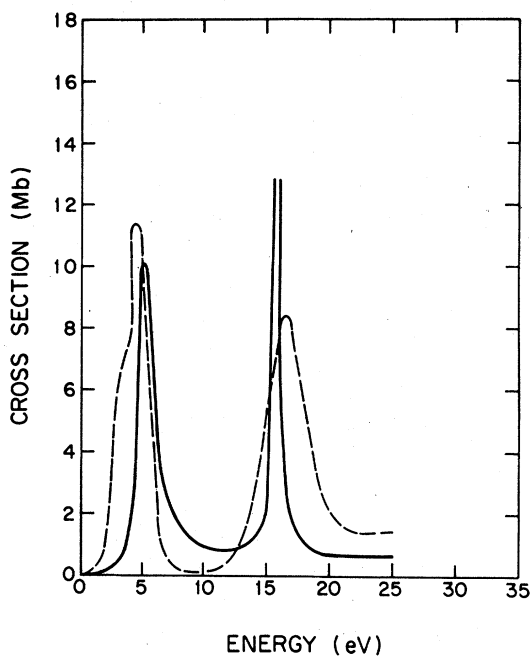


FIG. 3. Sulphur $L_{II,III}$ core spectrum. The solid curve is the calculated curve and is reduced by a factor of three. The dashed curve is the data of Ref. 4.

tail, are given in Table II. They are seen to compare closely to those of Connolly and Johnson,¹³ indicating that our Coulomb tail modification of the potential had only a small effect on the initial state. The transition state eigenvalues are consistently lower in energy, reflecting a more ionic potential. The only relevant difference is the different order of the $5t_{1u}$ and $2t_{2u}$ states. However, the separation of the eigenvalues involved is only 0.08 eV in the transition-state calculation of Connolly and Johnson and 0.10 eV in our calculation. This separation of eigenvalues is smaller than the resolution of the calculation. Moreover, from our calculation there are three states, the $1t_{2u}$, and $5t_{1u}$, and $3e_g$, within an interval of 0.58 eV. The transition-state calculations¹³ found these states to be in an interval of 0.76 eV. The smallest energy separation of peaks in the experimental energy-distribution curves (EDC's) is ~ 1.4 eV. SCF $MS-X\alpha$ transition-state calculations²⁰ of the binding energies of valence levels in molecules other than SF₆ are known to yield level spacing which differ from the experimentally determined spacings by $\sim 2-3$ eV. With such uncertainties in the calculated relative ordering of the valence levels the degenerate peak in SF₆ could be easily misidentified, and assignments of valence levels separated by less than 2 eV could be interchanged. Thus, a positive assignment of molecular orbitals to peaks in the EDC's may not be accomplished by

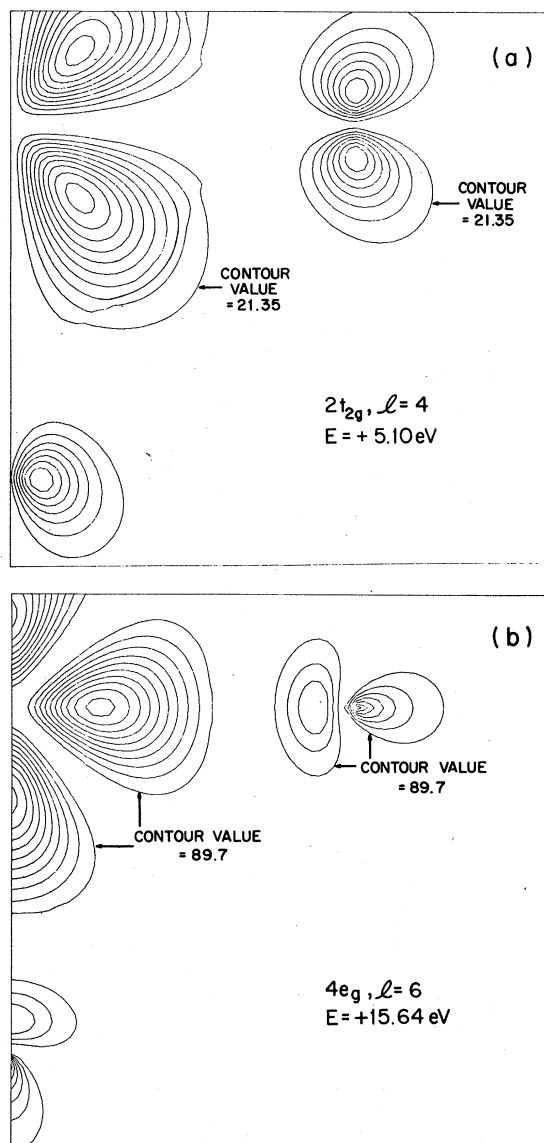


FIG. 4. Charge-density contour plots for photoemissions final states in a plane containing the sulphur atom and four fluorine atoms. Approximately $\frac{1}{4}$ of the plane is shown. The sulphur atom is in the upper-left-hand corner of each plot, with a fluorine below it and to its right. The remainder of the contours in this plane may be found by rotation about the center of the molecule (the sulphur atom). The increment in charge density between adjacent contours is 21.35 and 89.78 for (a) and (b), respectively. The absolute scale for the contours is fixed by Eq. (5). The discontinuity in the charge density in (a) occurs at the muffin-tin boundary.

an initial state calculated alone when the level separation is as small as in SF₆.

We have repeated the calculations of Sachenko *et al.* of the sulphur $L_{II,III}$ core-level cross sections. We show the results in Fig. 3 for later comparison with the valence spectra. The calculation

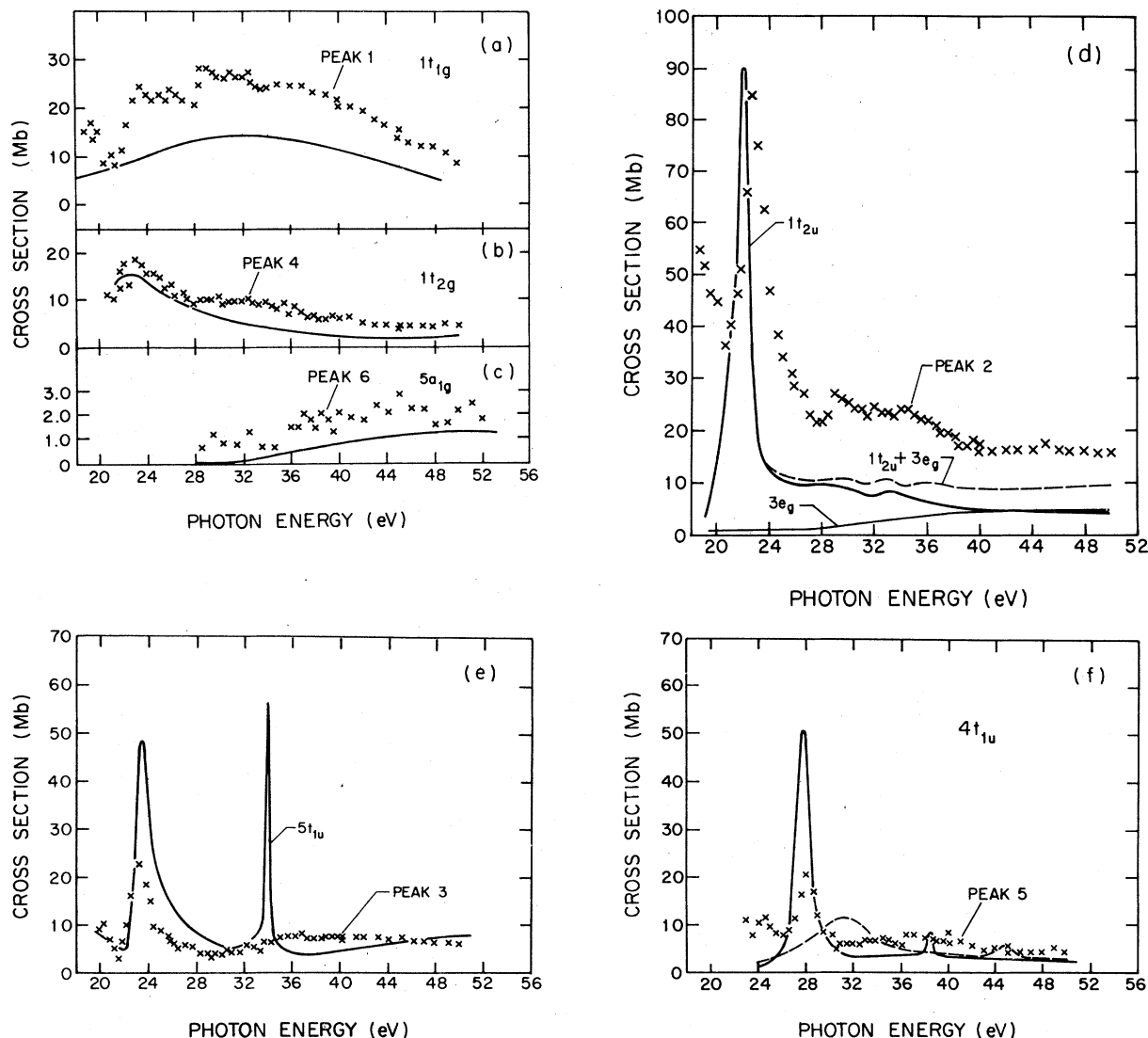


FIG. 5. Calculated and measured³ partial-photoionization cross sections for the five highest-lying valence levels of SF₆. Theoretical curves are plotted along with the data providing the best agreement between theory and experiment. The dashed curve in panel (e) is the calculated cross section for a non-self-consistent potential.

produces strong peaks at 5.1 and 15.6 eV, in general accord with experiment. (The spin-orbit induced splitting seen in the data is not reproduced by our nonrelativistic calculation.) As was also true for the earlier calculations, our peaks are too high and narrow as compared to experiment, a discrepancy due at least in part to the 0.5-eV resolution of the experiments.⁴ As was stated previously, the origin of the peaks are two very strong ($e^- + \text{SF}_6^+$) scattering resonances of t_{2g} and e_g symmetry. Dipole coupling between the sulfur p levels and resonances of these symmetries is allowed; the calculations show in addition that the overlap is large enough to produce very strong photoabsorption peaks.

Charge-density contour plots for final-state partial waves, $\Psi_{f,i}^{(i)}(\vec{r})$, which lead to the resonant behavior of the odd-parity states are shown in Fig. 4. The d -orbital character of the resonance within the sulphur sphere is seen in this figure. The normalization of the final state is chosen to have the asymptotic form

$$\Psi_f(\vec{r}) \xrightarrow{r \rightarrow \infty} \exp\{i[k \cdot \vec{r} - \gamma \ln(kr - \vec{k} \cdot \vec{r})]\} + f^{(-)}(\Omega) e^{-ikr}/r = \sum_i K_i^{(i)}(\vec{e}_r) \Psi_{f,i}^{(i)}(r), \quad (5)$$

$f^{(-)}(\Omega) e^{-ikr}/r$ is an incoming spherical wave, the $K_i^{(i)}$ are cubic harmonics, i denotes the symmetry type (e.g., t_{1u}, e_g , etc.) and $\gamma = e^2 m / \hbar^2 k$.

The photoemission cross section is a sum of contributions from partial waves as determined by the partial-wave decomposition of the final state in Eq. 5. In our calculation the partial waves which give the largest contribution to the resonances in the photoemission spectra of SF₆ are $4e_g$, $l = 6$ (the resonance calculated to be at 15.6 eV kinetic energy) and $2t_{2g}$, $l = 4$ (5.1 eV kinetic energy). It is clear from the charge-density plots in Fig. 4 that the resonances have pronounced spatial character within the frame of the molecule, just as for bound states. Thus, while a transition between a bound state and a resonance may be dipole allowed, the spatial characteristics of the states involved may result in small overlap and hence a small transition matrix element.

The computed and measured partial-photoionization cross sections for the seven highest-lying-valence levels are given in Fig. 5. Along with the theoretical curves, on each of the graphs we have plotted that experimental partial cross sections³ which, in our view, comes closest to being predicted by the particular theoretical curve with which it appears.

We first consider the four even-parity valence states ($5a_{1g}$, $1t_{2g}$, $1t_{1g}$, $3e_g$) and the three experimental peaks (1, 4, 6) that show no indication of coupling to the final state resonance. The measured cross section for peak 6 is very small (never greater than 3 Mb) and is structureless for $\hbar\omega \leq 50$ eV. The calculated cross sections for the $5a_{1g}$ level exhibit the same behavior. For this reason we believe that the assignment of $5a_{1g}$ to peak 6 is unambiguous. Plots of both the theoretical and experimental cross section are given in Fig. 5(c). The experimental cross sections for peaks 1 and 4 are shown in Figs. 5(a) and 5(b). Peak 4 is very well represented in shape and magnitude by the theoretical cross section for $1t_{2g}$. Peak 1 has the general shape of the theoretical cross section for $1t_{1g}$, and a similar magnitude as well. It does not seem likely that these assignments could be interchanged. The theoretical cross section for the remaining even parity level, $3e_g$, is shown in Fig. 5(d). It is clear that it has both the wrong magnitude and shape to account for either peak 1 or 4. Our conclusion for the even-parity states is, therefore, that the assignments proposed by Gustafsson³ are correct, and that the $3e_g$ level is hidden under a peak dominated by one of the other levels.

We now consider the odd-parity valence states ($4t_{1u}$, $5t_{1u}$, 15_{2u}) and the three peaks in the measured spectrum (2, 3, 5), which apparently couple to the final state resonances. The major questions regarding the odd-parity states is, firstly, whether they will exhibit the correct resonant behavior,

and secondly, whether it would be possible to clarify the assignments of peaks 2 and 3. At first glance it would appear that for calculations of the sort described here the answer to the first question would have to be negative. The fact that we employ the same potential for finding the final states for both the valence and core cross sections suggests that of necessity we must find two resonant peaks in both cases, in opposition to the data. This reasoning, however, is incomplete, since it neglects the possibility that while a transition may be dipole allowed on the basis of symmetry, the wave-function overlap may be so small as to render it weak or unobservable. We found that all three odd-parity states couple strongly to the t_{2g} resonance, whereas the $1t_{2u}$ couples negligibly, the $4t_{1u}$ couples weakly, and the $5t_{1u}$ couples very strongly to the e_g resonance. We will comment later on the implications of this state of affairs.

The overall magnitude and shape of the theoretical cross section for the $4t_{1u}$ level agrees moderately well with the experimental results for peak 5. This seems to confirm the assignment of Gustafsson.³ The large peak at $\hbar\omega = 28$ eV arises from the t_{2g} resonance and the smaller peak at 38 eV from the e_g resonance. We do not claim, although it is certainly possible, that the scatter in the data near 39 eV is a remnant of the high-lying resonance. Our calculations are unsuccessful in completing the assignments of $1t_{2u}$ and $5t_{1u}$. We show the theoretical cross sections for peak 2 with $1t_{2u}$ and with peak 3 with $5t_{1u}$ in Figs. 4(d) and 4(e), respectively. The association could have been interchanged. In addition, the theoretical curve for $5t_{1u}$ shows a very strong coupling to the e_g resonance, which is not at all indicated in the data.

We can draw no conclusion about which experimental peak contains the $3e_g$ level. Fig. 5(d) shows the result of adding the theoretical result for $3e_g$ to that for $1t_{2u}$, in accordance with the suggestion of Gustafsson. While the agreement is better, it is only marginally so. Thus, while the discussion above shows that it is the $3e_g$ level that is being masked, we cannot tell, on the basis of this work, where it is hidden.

The dashed line in Fig. 5(f) is the partial-photoionization cross section calculated, not from the self-consistent potential, but instead from the potential obtained by merely overlapping atomic orbitals. This "molecular potential" does not include charge transfer as in the self-consistent potential. Such charge transfer is the result of chemical interactions among the atoms comprising the molecule. For this non-self-consistent potential, both the $2t_{2g}$ and $4e_g$ resonance appear, though broadened and at higher energy. The existence of

TABLE III. $X\alpha$ total charge distribution (units of e).

	Self-consistent potential	Overlapped atomic potentials
Sulphur sphere	13.45	12.46
Fluorine sphere	7.24	7.41
Outer sphere	1.68	1.84
Intersphere region	11.45	11.25

the resonances is hence *not* dependent on charge transfer. The shift of levels to lower energy as the result of interatomic interactions is simply chemical bonding. The charge distribution for the self-consistent and non-self-consistent potentials is given in Table III. There is not the typical charge transfer into the fluorine spheres. This may be viewed as the result of competition for electrons among the six highly-electronegative fluorines and the somewhat electronegative sulphur.

These conclusions, obtained by considering ground-state properties, are somewhat at variance with the "two well potential" model discussed by Dehmer.¹ In that model it was assumed that the electronegativity of the fluorines would lead to a sulphur atom with net positive charge. At large distances from the molecule an electron would see the Coulomb attraction of the molecular ion. These two regions of net attraction would be separated by a barrier of negatively charged fluorines.

Our considerations of the final state indicate a two well potential, but of physical origin somewhat different from that discussed by Dehmer. Table III and Fig. 5(f) suggest (i) that these resonances exist even in the absence of charge transfer and (ii) that the charge transfer in SF_6 , as described by the self-consistent potential, actually is opposite to what would be necessary if it were to be a major reason for the existence of the resonances. One may remember that similar resonances also exist in molecular nitrogen,^{8,21} where of course, the bonding is covalent.

IV. CONCLUSIONS

The only qualitative disparity between the measured photoionization cross sections for the va-

lence levels of SF_6 and our calculation is the predicted double-resonance structure which we find for one of the odd-parity states and which does not appear to exist in the data. This disagreement is presumably the result of our having employed an inappropriate one-electron potential for calculating the final states. In view of the fact that the outgoing electron moves in the combined field of the neutral atom and the particular hole left behind, it is possible that when the correct hole field is employed the potential barriers responsible for the high-lying resonance will be modified. Studies to investigate this are underway. Alternatively, some subtle many-body effect may be involved.²²

In general, the single-electron model works well for calculating the various partial cross sections. The ability of the calculation to reproduce most qualitative and even many quantitative features of the photoemission spectra permits the identification of most levels by the scheme. Only where there are two closely-spaced levels, e.g., $5t_{1u}$ and $1t_{2u}$, with the same qualitative characteristics, is the identification uncertain.

ACKNOWLEDGMENTS

We wish to acknowledge many useful discussions with Dr. Natalie Holzwarth. The computer programs used for calculating the photoemission cross sections were based on programs of Dr. J. W. Davenport. We also wish to thank the staff of the David Rittenhouse Laboratory Computer Facility for their assistance and patience. This work was supported by the NSF through the University of Pennsylvania Materials Research Laboratory under Grant Nos. DMR77-10137, NSF/MRL-DMR78-80994-A01, and DMR 77-23420, and by a grant from the Research Corporation.

¹J. L. Dehmer, *J. Chem. Phys.* **56**, 4496 (1972).

²F. A. Cotton, *Chemical Applications of Group Theory* (Wiley-Interscience, New York, 1971).

³T. Gustafsson, *Phys. Rev. A* **18**, 1481 (1978).

⁴T. M. Zimkina and A. S. Vinogradov, *J. Phys. (Paris)* **32**, 3 (1971).

⁵K. Siegbahn, C. Nordling, G. Johansson, J. Hedman, P. F. Hedén, K. Hamrin, U. Gelius, T. Bergmark,

L. O. Werme, R. Manne, and Y. Baer, *ESCA Applied to Free Molecules* (North-Holland, Amsterdam, 1969).

⁶V. P. Sachenko, E. V. Polozhentsev, A. P. Kovtun, Yu. F. Migal, R. V. Vedrinski, and V. V. Kolesnikov, *Phys. Lett. A* **48**, 169 (1974).

⁷D. Dill and J. L. Dehmer, *J. Chem. Phys.* **61**, 692 (1974).

⁸J. W. Davenport, *Phys. Rev. Lett.* **36**, 945 (1976).

- ⁹W. von Niessen, L. S. Cederbaum, G. H. F. Diercksen, and G. Hohlneicher, *Chem. Phys.* **11**, 399 (1975).
- ¹⁰G. L. Bendazolli, P. Palmieri, B. Cadioli, and U. Pinelli, *Mol. Phys.* **19**, 865 (1970).
- ¹¹F. A. Gianturco, C. Guidotti, U. Lamanna, and R. Moccia, *Chem. Phys. Lett.* **10**, 269 (1971).
- ¹²D. P. Santry and G. A. Segal, *J. Chem. Phys.* **47**, 158 (1967).
- ¹³J. W. D. Connolly and K. H. Johnson, *Chem. Phys. Lett.* **10**, 616 (1971).
- ¹⁴N. Rosch, V. H. Smith, Jr., and M. H. Whangbo, *J. Am. Chem. Soc.* **96**, 5984 (1969).
- ¹⁵J. C. Slater, *Adv. Quantum Chem.* **6**, 1 (1972).
- ¹⁶K. H. Johnson, *Adv. Quantum Chem.* **7**, 143 (1973).
- ¹⁷J. C. Slater, *Quantum Theory of Matter*, 2nd ed. (McGraw-Hill, New York, 1968).
- ¹⁸K. Schwarz, *Phys. Rev. B* **5**, 2466 (1972).
- ¹⁹R. Latter, *Phys. Rev.* **99**, 510 (1955).
- ²⁰J. W. D. Connolly, H. Siegbahn, U. Gelius, and C. Nordling, *J. Chem. Phys.* **58**, 4265 (1973).
- ²¹J. L. Dehmer and D. Dill, *Phys. Rev. Lett.* **35**, 213 (1975).
- ²²Anthony F. Starace, *Phys. Rev. A* **2**, 118 (1970).
- ²³W. Lotz, *J. Opt. Soc. Am.* **60**, 206 (1970).